Competitive adsorption equilibria of CO$_2$ and CH$_4$ on a dry coal

**Stefan Ottiger · Ronny Pini · Giuseppe Storti ·
Marco Mazzotti**

Abstract Gases like CO$_2$ and CH$_4$ are able to adsorb on the coal surface, but also to dissolve into its structure causing the coal to swell. In this work, the binary adsorption of CO$_2$ and CH$_4$ on a dry coal (Sulcis Coal Province, Italy) and its swelling behavior are investigated. The competitive adsorption measurements are performed at 45 °C and up to 190 bar for pure CO$_2$, CH$_4$ and four mixtures of molar feed compositions of 20.0, 40.0, 60.0 and 80.0% CO$_2$ using a gravimetric-chromatographic technique. The results show that carbon dioxide adsorbs more favorably than methane leading to an enrichment of the fluid phase in CH$_4$. Coal swelling is determined using a high-pressure view cell, by exposing a coal disc to CO$_2$, CH$_4$ and He at 45 and 60 °C and up to 140 bar. For CO$_2$ and CH$_4$ a maximum swelling of about 4 and 2% is found, whereas He shows negligible swelling. The presented adsorption and swelling data are then discussed in terms of fundamental, thermodynamic aspects of adsorption and properties which are crucial for an ECBM operation, i.e. the CO$_2$ storage capacity and the dynamics of the replacement of CH$_4$ by CO$_2$.

Keywords Supercritical adsorption · Multicomponent · Carbon dioxide · Methane · Coal · Swelling

S. Ottiger · R. Pini · G. Storti · M. Mazzotti (✉)
Institute of Process Engineering, ETH Zurich, Sonneggstrasse 3, 8092 Zurich, Switzerland
e-mail: marco.mazzotti@ipe.mavt.ethz.ch

G. Storti
Institute for Chemical and Bioengineering, ETH Zurich, Wolfgang-Pauli-Str. 10, 8093 Zurich, Switzerland

1 Introduction

The atmospheric concentration of greenhouse gases has been rising steadily in the last years. Of particular concern are the emissions of carbon dioxide, methane and nitrous oxide, which have increased significantly due to human activities and exceed by far the pre-industrial values. The increase of carbon dioxide is mainly due to the use of fossil fuels, whereas those of methane and nitrous oxide are mainly due to agriculture. In the recently published summary for policymakers of the Intergovernmental Panel on Climate Change Fourth Assessment Report, it is stated that "most of the observed increase in globally averaged temperatures since the mid-20th century is very likely due to the observed increase in anthropogenic greenhouse gas concentrations" (IPCC 2007). Among these gases, CO$_2$ is considered the major contributor to global warming.

Therefore, in order to achieve the required reduction in CO$_2$ emissions, several actions have to be taken. Some of the options are to minimize emissions by reducing energy consumption and increasing the efficiency of energy generation or to switch to zero-CO$_2$ emission technologies such as renewable energies and nuclear energy. Capturing the CO$_2$ produced by current technologies, for example from a fossil fuel power plant, and storing it in a safe and permanent manner, i.e. CO$_2$ capture and storage (CCS), is another option, which could thus play an important role in the transition to the aforementioned zero-emission technologies (IPCC 2005). Possible storage sites are geological formations, i.e. water-bearing aquifers, depleted oil- and gas fields and unmineable coal seams.

In this work, we are focussing on a novel technology called Enhanced Coal Bed Methane recovery (ECBM), which allows recovering methane from a coal seam by carbon dioxide injection. Due to higher adsorptivity of carbon

dioxide with respect to methane, the injected carbon dioxide displaces the adsorbed methane. Ultimately, most of the methane is recovered and the coal seam contains mainly carbon dioxide, which remains there permanently separated from the atmosphere. ECBM is therefore attractive from two perspectives. On the one hand, if one is interested in the recovered methane as a fuel or a technical gas, ECBM allows also for a net CO_2 sequestration, thanks to the above mentioned high CO_2 adsorptivity. On the other hand, if the goal is that of storing CO_2 that has been captured, the ECBM operation allows also recovering methane, thus making CO_2 storage economically interesting in this case.

There have been so far only a few field tests in progress (Reeves et al. 2003; Van Bergen 2006; Wong et al. 2006; Yamaguchi et al. 2006; Quattrocchi et al. 2006). Nevertheless, our knowledge about the fundamental issues related to ECBM is still limited. Therefore, as a first step towards a better understanding of the process, three aspects are to be investigated: first, measurements of pure CO_2 adsorption are needed to estimate the CO_2 capacity of the coal seam and the storage potential. Secondly, data about competitive adsorption of CO_2 and CH_4 are a prerequisite to describe the adsorption/desorption dynamics in the coal seam during the displacement of methane by carbon dioxide. Thirdly, the influence of the CO_2 injection on coal swelling must be quantified precisely, because it controls the coal permeability hence the feasibility of the whole ECBM operation. In a recent paper, in the framework of a feasibility study for a CO_2–ECBM operation currently in progress, pure gas adsorption of CO_2 and CH_4 on coal was investigated (Ottiger et al. 2006). In this work, we are now focussing on the competitive adsorption of CO_2 and CH_4 on coal and on its swelling behavior.

Recently, high-pressure adsorption of pure and binary CO_2 and CH_4 on coal has received a lot of attention in the literature. For instance, the adsorption of pure CO_2 and CH_4 was measured on two types of Australian coals at three temperatures and up to 20 MPa (Bae and Bhatia 2006), as well as on dry and moisture-equilibrated Pennsylvanian coals (Krooss et al. 2002). The adsorption of binary and ternary mixtures of CO_2, CH_4 and N_2 on dry Australian coal has been measured and both the ideal and real adsorbed solution theory have been applied (Stevenson et al. 1991). Pure and multicomponent adsorption data of the same gases on wet U.S. coals were collected and described with different isotherms, namely a two-dimensional equation of state, the ideal adsorbed solution theory and the extended Langmuir isotherm (Arri et al. 1992; DeGance et al. 1993; Chaback et al. 1996). In addition, an extensive set of high-pressure adsorption data of CO_2, CH_4 and N_2 and their mixtures on three water-moistened coals, namely Fruitland, Tiffany and Illinois, was reported, and the data were described using a simplified local-density model (Fitzgerald et al. 2005;

Fitzgerald and Robinson 2006). The displacement of CH_4 adsorbed on coals by injecting either pure CO_2, pure N_2 or CO_2/N_2 mixtures was investigated on a dried Japanese coal sample (Shimada et al. 2005), and CO_2–CH_4 binary adsorption measurements on two types of Polish coal have also been reported (Ceglarska-Stefanska and Zarebska 2005). Finally, the adsorption of pure CO_2 and a flue gas (containing mainly nitrogen, carbon dioxide, hydrogen and methane) on a coal sample from the Silesian Basin in Poland in dry and wet state was recently investigated, showing that CO_2 was the most and CH_4 the second most preferred component adsorbed (Mazumder et al. 2006). However, there are also results which are in disagreement with the majority of the published literature that indicates CO_2 is more adsorbable than CH_4. Among these there are the data reported by Busch and coworkers, who measured single and binary adsorption of methane and carbon dioxide on dry Argonne premium coals (Busch et al. 2003) and on a variety of dry and moisture-equilibrated coal samples (Busch et al. 2006).

All the competitive adsorption data summarized above were obtained by applying a volumetric technique, in combination with the analysis of fluid phase composition by gas chromatography. In principle, there exist several other methods to determine gas mixture adsorption isotherms, among which are the gravimetric-chromatographic, the densimetric-gravimetric and the volumetric-gravimetric methods (Keller et al. 1999; Keller and Staudt 2005). All these three techniques rely on a gravimetric measurement, whereas the analysis of the fluid phase composition is carried out differently, namely by gas chromatography in the first case and by combining density and pressure with a suitable equation of state in the second and third case, respectively. The latter two methods differ in that the directly measured quantities are the density (Dreisbach et al. 2002) and the amount of gas fed to the system (Dreisbach et al. 1999), respectively. In this work, the gravimetric-chromatographic technique has been employed and the adsorption isotherms of pure CO_2 and CH_4, and of four binary mixtures of these gases on coal from the Sulcis Coal Province (Sardinia, Italy) were measured. Experiments have been performed at a temperature of 45 °C and at pressures up to 190 bar, i.e. at conditions which are representative for the conditions in the coal seam upon CO_2-ECBM operation.

The swelling of coal when exposed to different gases has been the subject of several studies and different techniques have been applied to estimate it. In his study, Reucroft measured with a dilatometer the swelling of different coal samples 1 cm long and 0.4 cm in diameter (Reucroft and Sethuraman 1987). A volume increase ranging from 0.75% to 4.18% was observed when exposing the samples to CO_2 at a pressure of 15 bar. Harpalani and Chen used strain gauges attached to the surface of a coal core of 3.8 cm in diameter to measure the changes in volume of the

sample with addition of CH_4 and He up to a pressure of 69 bar (Harpalani and Schraufnagel 1990). While for helium a volume decrease of about 0.09% was observed, using methane the volume increased by 0.5%. Using a similar technique, St. George and Barakat report coal volume shrinkage up to 4.5% and 2% when releasing the pressure from a coal sample previously saturated at 40 bar with CO_2 and CH_4, respectively. In the case of helium, the sample expanded slightly with the reduction of pressure (St. George and Barakat 2001). In the literature, two possible interpretations of the coal swelling are given. On the one hand, being a porous solid, the coal may expand because of the pure physical adsorption process. It is known that adsorption of a gas induces changes in the specific surface energy of a body and as a consequence the body deforms. The change in surface energy is thus accommodated by the change in elastic energy used for the deformation process (Scherer 1986; Pan and Connell 2007). On the other hand, coal is a glassy, strained, cross-linked macromolecular system and, as in the case of polymers, can uptake several organic solvents (Larsen 2004). It has been observed in an X-ray study that upon exposure to CO_2, the coal undergoes structure changes, which can be explained only by a dissolution mechanism of the CO_2 into the coal (Karacan 2003). Moreover, in another study a decrease in the coal's softening temperature with increasing CO_2 is reported (Larsen 2004). The plasticizing effect of CO_2 is a well known phenomenon in the polymer chemistry. All these aspects evidence the fact that, as in the case of a polymer, coal is absorbing the CO_2, causing the coal to swell. Therefore, the uptake process of CO_2 can be viewed as a combination of adsorption on the coal's surface and penetration (absorption) into the coal's matrix. Following this idea, Duda and coworkers used a multiple sorption model (including both adsorption and absorption mechanisms) to describe the behavior of coal when exposed to CO_2 and CH_4 (Milewska-Duda et al. 2000). It is worth noting that, as we will see later in the discussion section, different representations of the coal's uptake mechanisms of gases, i.e. only adsorption or a combination of ab- and adsorption, leads to significantly different interpretation of the adsorption isotherms. In this work, the effect of exposing a coal disc to an atmosphere of CO_2, CH_4 and He is investigated at temperatures of 45 and 60 °C and pressures up to 140 bar and the resulting swelling is determined using a high-pressure view cell.

The motivation for this study is three-fold: first, the literature on competitive adsorption of CO_2 and CH_4 on coal is not fully consistent, as mentioned above. Secondly, the specific adsorption and swelling properties of a coal that has not been characterized yet have to be determined experimentally anyhow since it is currently not possible to estimate them from corresponding data on other coal samples, though with a similar coal composition. Last but not least, measuring binary adsorption and swelling at super- and near-critical conditions represents a challenge from both a theoretical and a practical point of view.

2 Competitive adsorption of CO_2 and CH_4

2.1 Materials

In this study, as in our previous paper (Ottiger et al. 2006), a coal sample from the Monte Sinni coal mine (Carbosulcis, Cagliari, Italy) in the Sulcis Coal Province was used. The sample was drilled in July 2006 at a depth of about 500 m and preserved in a plastic bottle in air. Results of a thermogravimetric analysis (TGA) on another coal sample from the same mine showed a coal composition of 49.4% in fixed carbon content, 41.2% in volatile matter, 2.1% in ash and 7.3% in moisture (Ottiger et al. 2006). These values together with a vitrinite reflectance coefficient ($R_o \cong 0.7$) allow classifying the coal as high volatile C bituminous (Quattrocchi et al. 2006). For the adsorption measurements, the coal sample was ground and sieved to obtain particles with diameter between 250 and 355 μm. Subsequently, it was dried in an oven at 105 °C under vacuum for one day. The dried sample was split into two parts: the first fraction, $m_{10}^{coal} = 2.97$ g, was placed in the sample basket of the magnetic suspension balance, whereas the second fraction, $m_{20}^{coal} = 37.84$ g was loaded in the adsorption cell (see Fig. 1 and below).

The pure gases used in this study were obtained from Pangas (Dagmersellen, Switzerland), namely CO_2 and CH_4 at purities of 99.995% and He at a purity of 99.999%. Four cylinders containing carbon dioxide/methane mixtures of certified compositions were purchased from Pangas (Dagmersellen, Switzerland), that produced them using CO_2 and CH_4 at purities of 99.995%. The molar compositions of these gas mixtures are 20.0, 40.0, 60.0 and 80.0% CO_2, respectively. The critical properties of the pure adsorbates are as follows: $T_c(He) = 5.26$ K, $P_c(He) = 2.26 \times 10^5$ Pa, $\rho_c(He) = 69.3$ kg/m³; $T_c(CO_2) = 304.1$ K, $P_c(CO_2) = 73.7 \times 10^5$ Pa, $\rho_c(CO_2) = 467.6$ kg/m³; $T_c(CH_4) = 190.6$ K, $P_c(CH_4) = 46.0 \times 10^5$ Pa and $\rho_c(CH_4) = 162.7$ kg/m³.

2.2 Experimental set-up

The measurements reported in this study were performed in an experimental set-up that was developed and built in-house partially using commercially available components, a scheme of which is shown in Fig. 1. The heart of the set-up is a Rubotherm (Bochum, Germany) magnetic suspension balance which allows weight measurements with an absolute accuracy of 0.01 mg at pressures up to 450 bar and temperatures up to 250 °C. It consists of a permanent

Fig. 1 Setup for the gas mixture adsorption measurements. For better visibility, the calibrated void volume of the system is connected by *thick solid lines*
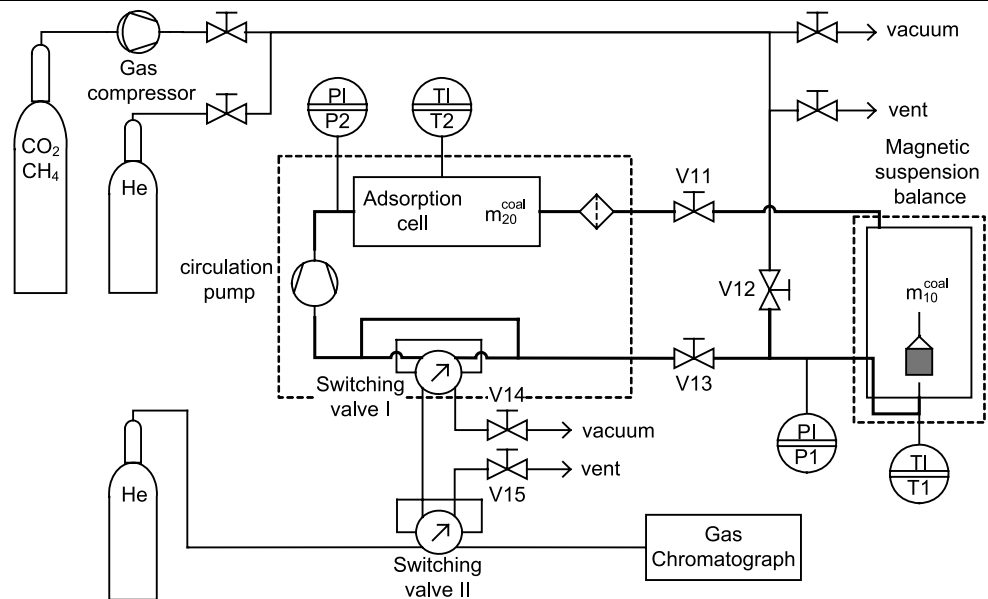
magnet to which a basket containing the sorbent and a titanium sinker element are attached. This permanent magnet is magnetically coupled to an electric magnet (located outside the measuring cell) which is connected to the control system. The distance between the two magnets is related to the weight of the elements connected to the permanent magnet. A key feature of the magnetic suspension balance is that the density of the bulk fluid can be measured directly by exploiting the presence of the titanium sinker element, whose mass and volume are known. The details about the measurement principle of the magnetic suspension balance have been described in detail elsewhere (Di Giovanni et al. 2001).

Beside the Rubotherm magnetic suspension balance, the experimental set-up consists of an auxiliary adsorption cell, a circulation pump and two switching valves. In the auxiliary adsorption cell, extra adsorbent is placed in order to amplify the change of gas phase composition upon adsorption thus improving the sensitivity and accuracy of the measuring system. The auxiliary cell has an inner diameter of 3.0 cm and a volume of about 110 cm^3; it was designed and built in-house for operation up to 300 bar and 200 °C, and it is equipped with two 50 µm frits at both ends to retain the coal. After the adsorption cell, an additional filter is placed with 20 µm pore size. The circulation pump was also designed and built in-house; it is a gear pump with a magnetic coupling and can be operated up to 700 bar and 200 °C (Zehnder 1992). The two switching valves D4C6W with electric actuators (VICI, Schenkon, Switzerland) allow analysis of the fluid phase composition by gas chromatography (HP 5890, Agilent Technologies, Basel, Switzerland), using helium as a carrier gas at a column flowrate of 25 mL/min. The species CO_2 and CH_4 are separated on a 20′ × 1/8″ SS column packed with Hayesep D of 100/120 mesh (Fluka, Buchs,

Switzerland) and detected with a TCD detector. The column and the detector are kept at a temperature of 100 °C and 240 °C, respectively. Finally, the set-up is completed by an air driven diaphragm type gas compressor Maximator DLE-15-30-2-GG-C (Ammann-Technik, Kölliken, Switzerland) and a vacuum pump (Trivac D4B, Leybold, Zurich, Switzerland).

The whole system is kept at the desired temperature by two liquid thermostats. The magnetic suspension balance is thermostated externally by a Julabo F25HE liquid thermostat (Seelbach, Germany). A Huber Polystat K 25-3 thermostat bath (Renggli, Rotkreuz, Switzerland) sets the temperature of the auxiliary adsorption cell, the circulation pump and the switching valve I. Additionally, the piping between these two parts of the set-up is heated electrically with a heating band (HST 8.0 m, Horst, Lorsch, Germany). This keeps the whole system at the same constant temperature. The temperature in the system can be measured with the thermocouples T1 and T2 with an accuracy of 0.1 °C. The thermocouple T1 (Rubotherm, Bochum, Germany) is located below the basket in the magnetic suspension balance, whereas the thermocouple T2 measures the temperature in the adsorption cell. The pressure in the system is measured with two pressure sensors P1 and P2. The first pressure sensor P1 is located close to the magnetic suspension balance (PMP 4010, Druck, Bad Nauheim, Germany) and can measure up to 400 bar with a reproducibility of 0.04%. The second pressure sensor P2 with an accuracy of 0.05% (PAA-35HTT, Keller, Winterthur, Switzerland) is located in the thermostat bath, and can be operated up to 300 bar and at temperatures between 20 and 80 °C.

2.3 Measurement procedure

The gas adsorption measurements are carried out as follows. First, the two coal samples of masses m_{10}^{coal} and m_{20}^{coal}, prepared as described in Sect. 2.1, are placed in the basket of the magnetic suspension balance and in the auxiliary adsorption cell, respectively. The magnetic suspension balance cell is disconnected from the part containing the auxiliary adsorption cell and it is evacuated at a temperature of 103 °C and the weight $\mathcal{M}_1^0$ is measured:

$$\mathcal{M}_1^0 = m^{met} + m_{10}^{coal}, \tag{1}$$

where m^{met} is the weight of the lifted metal parts. Then, the corresponding volume V^0 is determined by filling the measuring cell with helium at 99 °C and 183 bar using the following equation:

$$V^0 = V^{met} + V_{10}^{coal} = \frac{\mathcal{M}_1^0 - \mathcal{M}_1(\rho_{He}^b, T)}{\rho_{He}^b}, \tag{2}$$

where $\mathcal{M}_1(\rho_{He}^b, T)$ represents the weight measured in helium at the density ρ_{He}^b and the temperature T. The quantities m^{met} and V^{met}, i.e. the weight and volume of the metal parts, are known from a previous measurement with the empty sample basket at the same conditions. The initial volume of the coal in the balance is then directly obtained as a difference, i.e. $V_{10}^{coal} = V^0 - V^{met}$. However, the adsorption experiments are performed not only with the coal in the magnetic suspension balance, but also with the coal located in the auxiliary cell. Therefore, the total initial coal volume V_0^{coal} can be easily calculated from the total mass of both coal samples $m_0^{coal} = m_{10}^{coal} + m_{20}^{coal}$ by assuming proportionality as:

$$V_0^{coal} = \frac{m_0^{coal}}{m_{10}^{coal}} V_{10}^{coal}. \tag{3}$$

Here, it is worth noting that this measurement under helium is based on the assumption that helium does neither adsorb on the coal sample nor sorb in the coal matrix, therefore leading to no coal swelling. This assumption is fulfilled since helium adsorption on coal can be neglected (Ottiger et al. 2006), whereas the degree of swelling of coal under helium is also negligible (see Sect. 3).

After evacuating the whole system for two days at a temperature of 77 °C, the gas mixture to be adsorbed is brought to the desired pressure with the gas compressor and admitted to the system by opening valve V12 (see Fig. 1). The adsorption of the gas on the adsorbent leads to a change in the gas phase composition, and recirculation through the system is needed to guarantee attainment of phase equilibrium, i.e. usually after about 24 to 36 hours. Although the circulation pump can be operated at very low flow rates, it is switched

off for a few hours after reaching equilibrium, in order to obtain a precise weight measurement.

With the circulation pump running again, the composition of the fluid phase is determined by analyzing a small sample of it by gas chromatography. The sampling is carried out with the help of the two switching valves. Switching valve I is equipped with an external sampling loop of 20.5 μL and samples the gas at high pressure, which is released into the previously evacuated volume between valves V14 and V15. After expanding the gas mixture to atmospheric pressure, a gas sample is injected into the gas chromatograph by switching valve II, which is equipped with an external sample loop of 74.2 μL. This procedure allows injecting to the gas chromatograph always about the same amount of gas, independent of the pressure in the adsorption system; it is repeated at least five times for each measurement in order to check reproducibility. Using the four certified gas mixtures (see Sect. 2.1), a calibration was carried out prior to the measurements, thus relating the CH_4 mass fraction, w_{CH_4}, to the CH_4 peak area fraction, a_{CH_4}, through a polynomial function. The mole fraction y_i of component i in the mixture can be obtained as

$$y_i = \frac{\frac{w_i}{M_{m,i}}}{\sum_{i=1}^N \frac{w_i}{M_{m,i}}}, \tag{4}$$

where $M_{m,i}$ and N are the molar mass of component i and the number of components in the mixture, respectively.

When the fluid phase composition has been determined, additional gas mixture is admitted, the system is brought to a new pressure level, and the procedure described above is repeated. After maximally three to four loading steps, the system is evacuated for at least three hours before admitting additional gas to the system in order to limit the accumulation of experimental errors.

2.4 Evaluation of the molar excess amount adsorbed and sorbed

When the coal is brought into contact with the gas mixture, CO_2 and CH_4 do not only get adsorbed on the coal surface, but they are also absorbed in the coal matrix, thus causing the coal to swell. Therefore, the balance signal $\mathcal{M}_1(\rho^b, T)$ must take both adsorption and sorption mechanisms into account and can be written as

$$\mathcal{M}_1(\rho^b, T) = m^{met} + m_{10}^{coal} + m_1^a + m_1^s$$
$$- \rho^b \left(V^{met} + V_{10}^{coal} + V_1^a + V_1^s \right), \tag{5}$$

where m_1^a and m_1^s are the masses adsorbed and sorbed on coal sample 1, respectively. V_1^a is the volume of the adsorbed phase on coal sample 1, whereas V_1^s represents the volume

of the sorbed phase, i.e. the volume increase of coal sample 1 due to sorption.

The surface excess mass adsorbed m^{ex} is defined as the difference between the actual absolute amount adsorbed and the amount that would be present in the adsorbed phase if it had the same density as the bulk phase (Sircar 1985a). Therefore, for a homogeneous surface, the total excess mass adsorbed m^{ex} can be expressed as

$$m^{ex} = A \int_0^\infty [\rho(z) - \rho^b] dz = \int_0^\infty [\rho(z) - \rho^b] dV, \quad (6)$$

where A is the adsorbent surface area, $\rho(z)$ is the mass density as a function of the coordinate z perpendicular to the adsorbent surface. Using this definition, the total excess mass m_1^{ex} adsorbed on coal sample 1 located in the magnetic suspension balance can be obtained by solving the integral in (6) over the volume of the adsorbed phase V_1^a:

$$m_1^{ex} = m_1^a - \rho^b V_1^a. \quad (7)$$

Consequently, (5) can be reformulated by inserting (1) and (7):

$$m_1^{eas}(\rho^b, T) \equiv m_1^{ex} + m_1^s - \rho^b V_1^s$$
$$= \mathcal{M}_1(\rho^b, T) - \mathcal{M}_1^0 + \rho^b \left(V^{met} + V_{10}^{coal} \right), (8)$$

where the excess mass adsorbed and sorbed $m_1^{eas}(\rho^b, T)$ is defined as the sum of the excess adsorption m_1^{ex} and a sorption term corrected for the buoyancy $m_1^s - \rho^b V_1^s$. The right-hand side of (8) contains only measurable variables and therefore $m_1^{eas}(\rho^b, T)$ is the truly measurable quantity. It is worth pointing out that under the assumption that the gas mixture did only adsorb on the coal and does neither sorb in the coal matrix and nor swell the coal, m_1^{eas} would be equal to the excess mass adsorbed m_1^{ex}. This assumption is reasonable for example for the adsorption of CO_2 on standard commercial adsorbents such as zeolites, silica gel or activated carbon (Hocker et al. 2003; Pini et al. 2006). In our previous publication, we have applied the same assumption for the adsorption of pure CO_2 and CH_4 adsorption measurements on coal from the Sulcis Coal Province (Ottiger et al. 2006). However, it is well known that the coal changes its volume upon contacting with CO_2 and CH_4, due to sorption in the coal matrix, leading to the breakdown of this assumption. Therefore, the excess mass adsorbed and sorbed $m_1^{eas}(\rho^b, T)$ is the actually measured quantity if no correction is applied to account for sorption and swelling. The details about the practicability and necessity of such a correction will be discussed in detail in Sect. 4.

In the case of a pure gas, the experimental results are measured in the magnetic suspension balance only and are reported in terms of the molar excess adsorption and sorption per unit mass of coal

$$n^{eas}(\rho^b, T) = n^{ex} + n^s - \rho^b \frac{V_1^s}{M_m m_{10}^{coal}} = \frac{m_1^{eas}(\rho^b, T)}{M_m m_{10}^{coal}}, \quad (9)$$

where n^{ex} and n^s correspond to the molar excess adsorption and the molar sorption per unit mass of coal, respectively.

In the case of a mixture, the experiments are performed in the whole system including the auxiliary cell, where the same gas mixture adsorbs on the second coal sample of mass m_{20}^{coal}. Therefore, the total excess mass $m^{eas}(\rho^b, T)$ adsorbed and sorbed on both coal samples of total weight $m_0^{coal} = m_{10}^{coal} + m_{20}^{coal}$ is obtained by multiplying the total excess mass $m_1^{eas}(\rho^b, T)$ adsorbed and sorbed on coal sample m_{10}^{coal} by a proportionality factor, i.e.:

$$m^{eas}(\rho^b, T) \equiv m^{ex} + m^s - \rho^b V^s = \frac{m_0^{coal}}{m_{10}^{coal}} m_1^{eas}(\rho^b, T), \quad (10)$$

where m^s and V^s represent the amount of gas sorbed on both coal masses and the volume of the corresponding sorbed phase, respectively.

In order to determine the amount of gas fed to the system, a mass balance over the gas present in the system is needed. For this purpose, using the definition in (6), the total excess mass adsorbed m^{ex} can be recast as:

$$m^{ex} = m^a - \rho^b V^a = m^{feed} - m^s - \rho^b V^{void}, \quad (11)$$

where the two different expressions are obtained by solving the integral in (6) over the volume of the adsorbed phase V^a and over the void volume V^{void} accessible to the gas when the coal is in its swollen state, respectively. The quantities m^a and m^{feed} represent the absolute amount adsorbed and the total amount of gas fed to the system, respectively. V^{void} is related to the void volume with the coal in its unswollen state V_0^{void} by subtracting the volume of the sorbed phase V^s:

$$V^{void} = V_0^{void} - V^s. \quad (12)$$

The void volume V_0^{void} is known from a calibration prior to the adsorption measurements (see Appendix A). Therefore, the amount of gas fed m^{feed} is easily obtained by solving (11), replacing V^{void} using (12) and introducing the definition of $m^{eas}(\rho^b, T)$ given in (10):

$$m^{feed} = m^{ex} + m^s + \rho^b V^{void}$$
$$= m^{eas}(\rho^b, T) + \rho^b V_0^{void}. \quad (13)$$

At this point, it is worth noting that, as can be seen in (13), m^{feed} depends on the excess mass adsorbed and sorbed $m^{eas}(\rho^b, T)$, the density ρ^b and the void volume V_0^{void}, i.e.

quantities that can all be determined experimentally without knowing the exact degree of swelling of the coal, therefore the value of m^{feed} is independent of swelling.

For the determination of the individual adsorption, (6) can be written for all species present, and the surface excess mass adsorbed m_i^{ex} of component i can be written as

$$m_i^{\text{ex}} = A \int_0^\infty [\rho_i(z) - \rho_i^{\text{b}}] \mathrm{d}z, \tag{14}$$

where $\rho_i(z)$ is the mass density of component i, whereas ρ_i^{b} is its bulk density. Based on this definition, the following mass balances for each component i in the mixture can be written:

$$\begin{aligned} m_i^{\text{ex}} &= m_i^{\text{a}} - w_i^{\text{b}} \rho^{\text{b}} V^{\text{a}} \\ &= w_i^{\text{feed}} m^{\text{feed}} - m_i^{\text{s}} - w_i^{\text{b}} \rho^{\text{b}} V^{\text{void}}, \end{aligned} \tag{15}$$

where w_i^{feed} and w_i^{b} are the mass fractions of components i in the feed (which are known) and in the bulk fluid phase at equilibrium conditions (which are measured by GC), respectively. The individual excess mass adsorbed and sorbed $m_i^{\text{eas}}(\rho^{\text{b}}, T)$ is then obtained by solving (15) and replacing V^{void} using (12):

$$\begin{aligned} m_i^{\text{eas}}(\rho^{\text{b}}, T) &\equiv m_i^{\text{ex}} + m_i^{\text{s}} - w_i^{\text{b}} \rho^{\text{b}} V^{\text{s}} \\ &= w_i^{\text{feed}} m^{\text{feed}} - w_i^{\text{b}} \rho^{\text{b}} V_0^{\text{void}}. \end{aligned} \tag{16}$$

Here, it is worth mentioning that, according to the calculation described above, only the composition w_i^{feed} and not the exact total amount of gas m^{feed} fed to the system must be known a priori, since the latter is obtained through the mass balance given by (13).

As in the case of pure gas adsorption, the experimental results of the gas mixture adsorption experiments are reported in terms of the molar excess adsorption and sorption n_i^{eas} of component i per unit mass of coal:

$$\begin{aligned} n_i^{\text{eas}}(\rho^{\text{b}}, T) &= n_i^{\text{ex}} + n_i^{\text{s}} - w_i^{\text{b}} \rho^{\text{b}} \frac{V^{\text{s}}}{M_{\text{m},i} m_0^{\text{coal}}} \\ &= \frac{m_i^{\text{eas}}(\rho^{\text{b}}, T)}{M_{\text{m},i} m_0^{\text{coal}}}, \end{aligned} \tag{17}$$

where n_i^{ex} and n_i^{s} correspond to the molar excess adsorption and the molar sorption of component i per unit mass of coal, respectively. Finally, the total molar excess n^{eas} adsorbed and sorbed per mass of coal is equal to the sum of the molar excesses of all species:

$$n^{\text{eas}}(\rho^{\text{b}}, T) = \sum_{i=1}^{N} n_i^{\text{eas}}(\rho^{\text{b}}, T) \quad (i = \text{CO}_2, \text{CH}_4). \tag{18}$$

(a)

(b)
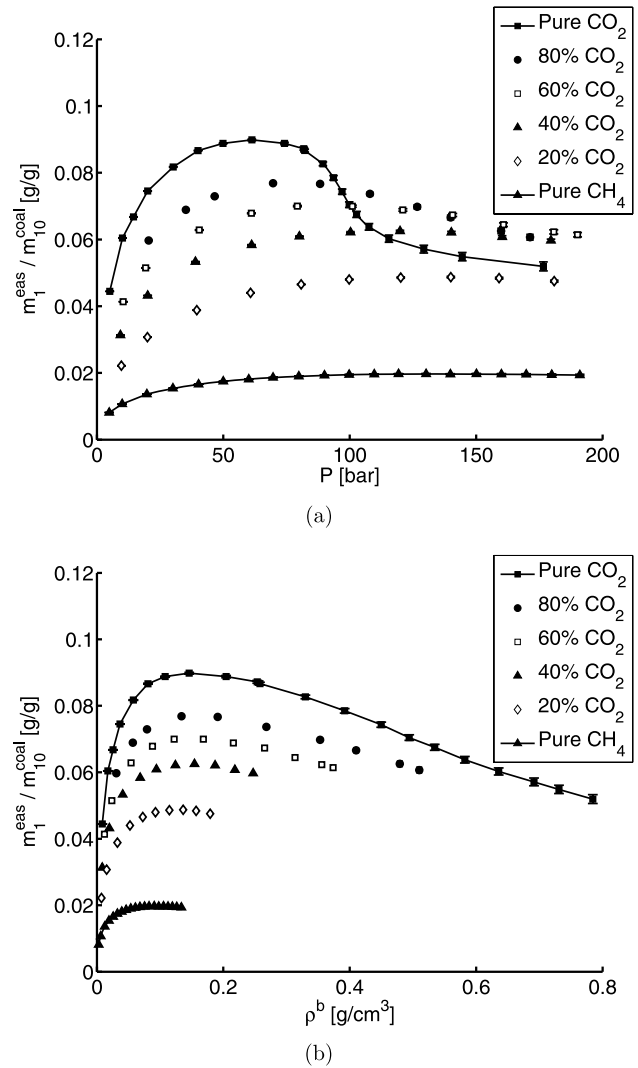
Fig. 2 Excess mass adsorbed and sorbed per unit mass of coal $m_1^{\text{eas}}/m^{\text{coal}}$ for pure CO_2, pure CH_4 and their mixtures on Sulcis coal at a temperature of 45 °C and different feed composition as a function of (**a**) pressure P and (**b**) density ρ^{b}. The data points of the pure CO_2 and CH_4 isotherms are connected to guide the eye. These results were all obtained from the balance signal only and are independent of the gas composition analysis in the case of the mixture

2.5 Results

The adsorption experiments have been performed at a temperature of 45 °C and at pressures up to 190 bar. These conditions are representative of those of the coal seam, since 45 °C is a temperature reached in the Sulcis Coal Province at about 500 m depth, where the coal sample investigated in this work was drilled, and the hydrostatic pressure is about 50 bar (Ottiger et al. 2006). Optimal conditions for an ECBM application are expected at even larger depths, namely between 800 and 1000 m, where temperatures up to about 70 °C and hydrostatic pressures up to about 100 bar can be reached.

Table 1 Experimental excess adsorption and sorption data of pure CO_2 on coal from the Sulcis Coal Province at 45 °C

P [bar]	ρ_m^b [mol/L]	n^{eas} [mmol/g]
5.1	0.20	1.010
10.1	0.40	1.373
14.5	0.58	1.517
20.1	0.83	1.693
30.2	1.31	1.857
40.0	1.84	1.968
49.9	2.46	2.017
61.3	3.32	2.041
74.2	4.64	2.017
81.8	5.76	1.982
82.2	5.86	1.969
89.4	7.50	1.878
93.6	8.91	1.783
97.0	10.22	1.689
99.8	11.23	1.601
102.7	12.14	1.534
107.6	13.23	1.449
115.5	14.44	1.369
129.3	15.71	1.297
144.5	16.61	1.246
176.6	17.83	1.180

Table 2 Experimental excess adsorption and sorption data of pure CH_4 on coal from the Sulcis Coal Province at 45 °C

P [bar]	ρ_m^b [mol/L]	n^{eas} [mmol/g]
4.9	0.19	0.507
10.0	0.38	0.665
19.8	0.77	0.849
30.1	1.18	0.959
40.2	1.60	1.033
50.0	2.02	1.088
60.1	2.46	1.128
69.7	2.88	1.160
79.9	3.34	1.184
90.0	3.80	1.202
99.8	4.25	1.213
109.7	4.71	1.221
119.3	5.15	1.226
130.2	5.66	1.228
139.8	6.10	1.222
150.1	6.57	1.226
160.0	7.01	1.222
169.8	7.44	1.218
179.9	7.88	1.212
191.0	8.34	1.207

Figure 2(a) shows the total excess mass adsorbed and sorbed m_1^{eas} divided by the mass of the coal sample m_{10}^{coal} for the pure gases CO_2 and CH_4 and their mixtures as a function of the pressure P. The excess mass adsorbed and sorbed m_1^{eas} was calculated through (8). These results show directly measurable quantities hence they depend on the balance signal only and are independent of the gas chromatography analysis. For pure CO_2, the isotherm first increases with pressure and then decreases following a curved behavior. For pure CH_4, the excess adsorbed and sorbed amount is significantly smaller, it increases with pressure and then decreases only slightly at the upper end of the explored pressure range. At low pressures, the excess isotherms of the mixtures lie between the two of the pure gases; starting from the pure methane isotherm, the excess increases with increasing CO_2 content in the feed. This is true until a pressure of about 100 bar, where the isotherms containing large amounts of CO_2 intersect with each other, particularly with the pure CO_2 isotherm. This is due to the phase behavior of carbon dioxide whose critical temperature is near ambient conditions and much closer to the measurement temperature than the one of methane. In fact, if the same data are plotted as a function of the density of the bulk fluid phase, ρ^b, as in Fig. 2(b), the crossover is not visible anymore in the investigated density range. After reaching the maximum, a typical linear descending part of the excess isotherm

can be observed for the isotherms with large CO_2 content in the feed. Note that the mixtures that contain more CO_2 reach higher density levels although the maximum pressure is about 190 bar in all cases.

The experimental data of pure CO_2 and CH_4 adsorption on coal from the Sulcis Coal Province are reported in Tables 1 and 2. The molar excess adsorption and sorption isotherms are slightly lower than the corresponding isotherms reported earlier (Ottiger et al. 2006), where the results were interpreted in terms of the molar excess adsorption n^{ex}, assuming that the coal does not swell. The difference between the isotherms is about 5% in the case of carbon dioxide and about 15% in the case of methane when considering the maximum of the isotherm. This may be due to the fact that the coal sample used in this study was drilled in the same coal mine, but not at the same time and the same precise location. Therefore, the extrapolation of the results presented in this work to the whole coal seam, as all results of this type based on a small sample, should be done cautiously.

Table 3 reports the experimental data for the adsorption of the CO_2/CH_4 mixtures that have been obtained through the mass balances described in Sect. 2.4. Figures 3(a) to 3(d) show the molar excess adsorption and sorption n_i^{eas} of each component i in the mixture per unit mass of coal plotted against the pressure P for the four gas mixtures of certified feed composition. The error bars were determined through

Table 3 Experimental excess adsorption and sorption data of CO_2/CH_4 mixtures on coal from the Sulcis Coal Province at 45 °C. The gas phase composition was determined by gas chromatography

$y_{CO_2}^{feed}$ [–]	P [bar]	$y_{CO_2}^{b}$ [–]	ρ_m^b [mol/L]	$n_{CO_2}^{eas}$ [mmol/g]	$n_{CH_4}^{eas}$ [mmol/g]
0.200	9.7	0.118	0.37	0.335	0.463
	20.0	0.136	0.78	0.494	0.558
	39.5	0.157	1.59	0.652	0.630
	60.8	0.166	2.53	0.774	0.620
	80.8	0.174	3.48	0.820	0.650
	99.8	0.178	4.40	0.849	0.663
	120.2	0.182	5.43	0.852	0.691
	140.0	0.184	6.43	0.873	0.641
	159.1	0.186	7.39	0.881	0.600
	180.9	0.187	8.42	0.893	0.513
0.400	9.3	0.287	0.35	0.595	0.319
	20.1	0.320	0.79	0.846	0.372
	39.0	0.347	1.59	1.065	0.400
	61.2	0.364	2.61	1.177	0.409
	80.1	0.372	3.57	1.233	0.415
	100.3	0.377	4.67	1.272	0.383
	119.9	0.381	5.78	1.278	0.390
	140.2	0.384	6.98	1.282	0.353
	160.3	0.387	8.13	1.250	0.357
	179.6	0.388	9.19	1.230	0.349
0.600	10.4	0.495	0.40	0.874	0.179
	19.3	0.530	0.76	1.089	0.219
	40.5	0.559	1.71	1.344	0.229
	61.1	0.571	2.75	1.463	0.216
	79.3	0.577	3.80	1.524	0.181
	101.0	0.582	5.21	1.539	0.140
	121.0	0.585	6.66	1.526	0.105
	140.7	0.589	8.16	1.482	0.130
	160.8	0.591	9.63	1.422	0.114
	180.7	0.592	10.91	1.374	0.113
	190.1	0.592	11.46	1.365	0.083
0.800	20.5	0.758	0.83	1.328	0.079
	35.2	0.772	1.51	1.537	0.080
	46.6	0.778	2.10	1.628	0.080
	69.7	0.786	3.52	1.723	0.064
	88.3	0.791	5.01	1.711	0.084
	108.0	0.794	7.02	1.645	0.079
	126.7	0.795	9.22	1.563	0.062
	139.9	0.796	10.71	1.490	0.063
	159.9	0.797	12.51	1.410	0.031
	171.3	0.797	13.31	1.368	0.030

the method of error propagation, the details of which are presented in Appendix B. The individual and total excess isotherms increase with pressure and then decrease after reaching a maximum for all investigated conditions, the only exception being CO_2 in Fig. 3(a) where its content in the feed is only 20%. The individual excess adsorbed and sorbed
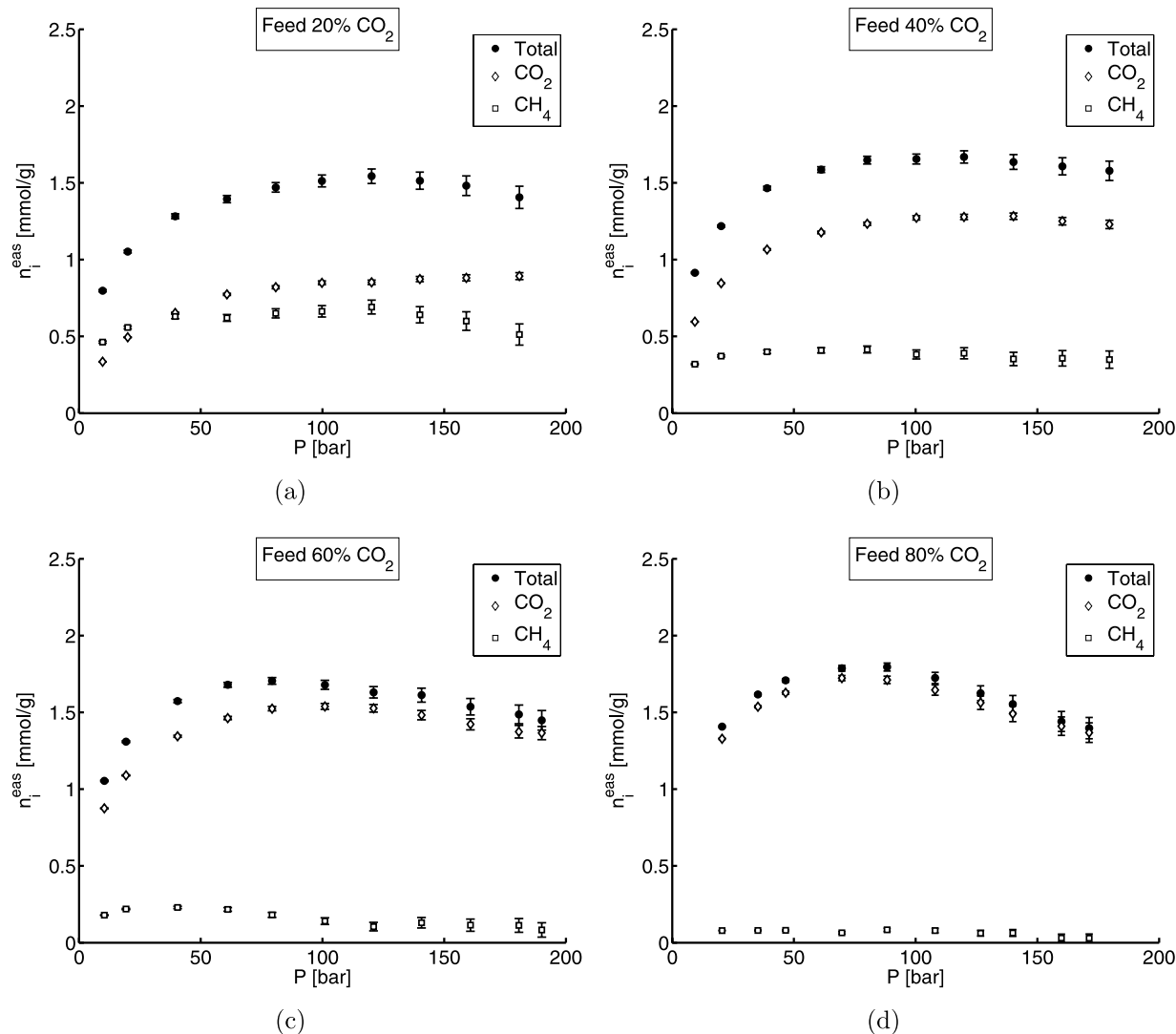
Fig. 3 Molar excess adsorption and sorption n_i^{eas} of component i per unit mass of Sulcis coal at a temperature of 45 °C as a function of the system pressure P. Feed compositions: (**a**) 20% CO_2, 80% CH_4; (**b**) 40% CO_2, 60% CH_4; (**c**) 60% CO_2, 40% CH_4; (**d**) 80% CO_2, 20% CH_4. $n_{CO_2}^{eas}$, $n_{CH_4}^{eas}$ and n^{eas} represent the CO_2, CH_4 and total molar excess adsorption and sorption, respectively

amounts are always larger for CO_2 than for CH_4, again with the exception of a 20% CO_2 feed at low pressure, i.e. less than 40 bar.

Figure 4 shows the CO_2 mole fraction in the bulk fluid phase, $y_{CO_2}^b$ (measured through GC), as a function of the pressure for the four mixture experiments. The horizontal lines represent the CO_2 mole fraction in the feed mixture $y_{CO_2}^{feed}$. In all four cases, $y_{CO_2}^b$ is always smaller than $y_{CO_2}^{feed}$. This indicates that CO_2 is preferentially adsorbed compared to methane at all pressures resulting in a reduced mole fraction of CO_2 in the fluid phase at equilibrium with respect to the feed. The CO_2 mole fraction in the fluid phase increases with increasing pressure and approaches asymptotically the feed mole fraction. This is because the ratio of the hold up in the fluid phase to the amount adsorbed increases also
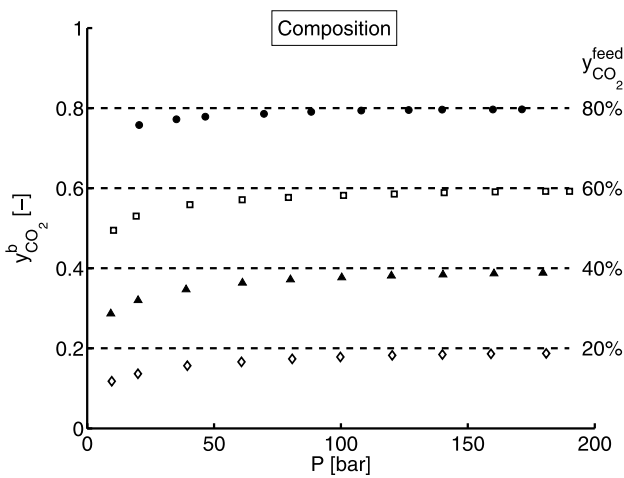
with increasing pressure, thus leading to a smaller change in composition due to preferential adsorption of carbon dioxide over methane.

Due to the large difference in molar weight between the two adsorbates, the density of the fluid phase ρ^b is much larger for mixtures containing large amounts of carbon dioxide, as observed in Fig. 2(b). Therefore, it is worth comparing the different isotherms at a constant molar bulk density. Since the composition of the bulk fluid phase y_i^b is known, the bulk density ρ^b can be transformed into the molar bulk density ρ_m^b through the following equation

$$\rho_m^b = \frac{\rho^b}{\sum_{i=1}^N M_{m,i} y_i^b}, \tag{19}$$

Table 4 Experimental swelling data of pure CO_2, CH_4 and He on a coal disc from the Sulcis Coal Province. The data is sorted with increasing pressure, distinguishing between the first and second exposure of the coal disc

Fluid	T [°C]	P [bar]	s [–]	Fluid	T [°C]	P [bar]	s [–]
CO_2	45	13	0.015	CO_2	60	31	0.022
		30	0.027			59	0.031
		44	0.030			98	0.034
		61	0.034	CH_4	45	41	0.016
		78	0.039			78	0.020
		94	0.038			114	0.022
		111	0.042			17	0.009
		128	0.042			35	0.011
		27	0.025			56	0.014
		60	0.034			76	0.017
		99	0.037			97	0.017
		112	0.038			116	0.020
	60	17	0.016	He	45	14	0.002
		35	0.023			40	0.000
		57	0.028			69	−0.001
		77	0.029			99	−0.001
		95	0.030			121	−0.003
		112	0.030				

Fig. 4 CO_2 mole fraction in the bulk fluid phase $y^b_{CO_2}$ at a temperature of 45 °C as a function of the pressure P. The horizontal lines represent the four different CO_2 mole fraction in the feed mixture $y^{feed}_{CO_2}$

where the denominator represents the mean molecular weight of the gas phase. Figures 5(a) and 5(b) show the molar excess adsorption and sorption $n^{eas}_{CO_2}$ and $n^{eas}_{CH_4}$ of CO_2 and CH_4 per unit mass of coal as a function of the molar bulk density ρ^b_m. Figure 5(c) shows the total molar excess adsorption and sorption per unit mass of coal n^{eas}, which is the sum of the two. The excess adsorbed and sorbed amounts of both CO_2 and CH_4 decrease with decreasing concentration of the specific compound in the feed. However, the reduction in excess adsorption and sorption is much stronger for the less adsorbing methane than for carbon dioxide, which is also a sign of the preferential adsorption of carbon dioxide over methane.

3 Swelling of coal

3.1 Materials and experimental set-up

The coal sample used for the swelling experiments was taken in the same coal mine as in the competitive adsorption measurements, i.e. the Monte Sinni coal mine (Carbosulcis, Cagliari, Italy) in the Sulcis Coal Province, however not at the same precise time and location. The coal sample was drilled in December 2004 at a depth of about 500 m, and preserved in a plastic bottle in air (Ottiger et al. 2006). From the coal block, a coal disc of about 22 mm in diameter was drilled with its two faces cut parallel. A disc shape was chosen as a compromise between measurement precision and equilibration time when the coal is exposed to a fluid. Prior to the swelling experiments, the coal disc was dried in an oven under vacuum at a temperature of 105 °C for two days in order to remove any pre-adsorbed moisture.

The swelling experiments were performed in a high-pressure view cell, which has been used in the past to study the expansion of polymers (Rajendran et al. 2005; Bonavoglia et al. 2006). The view cell is a cylindrical vessel and has a volume of about 50 cm³. Circular sapphire

(a)

(b)

(c)
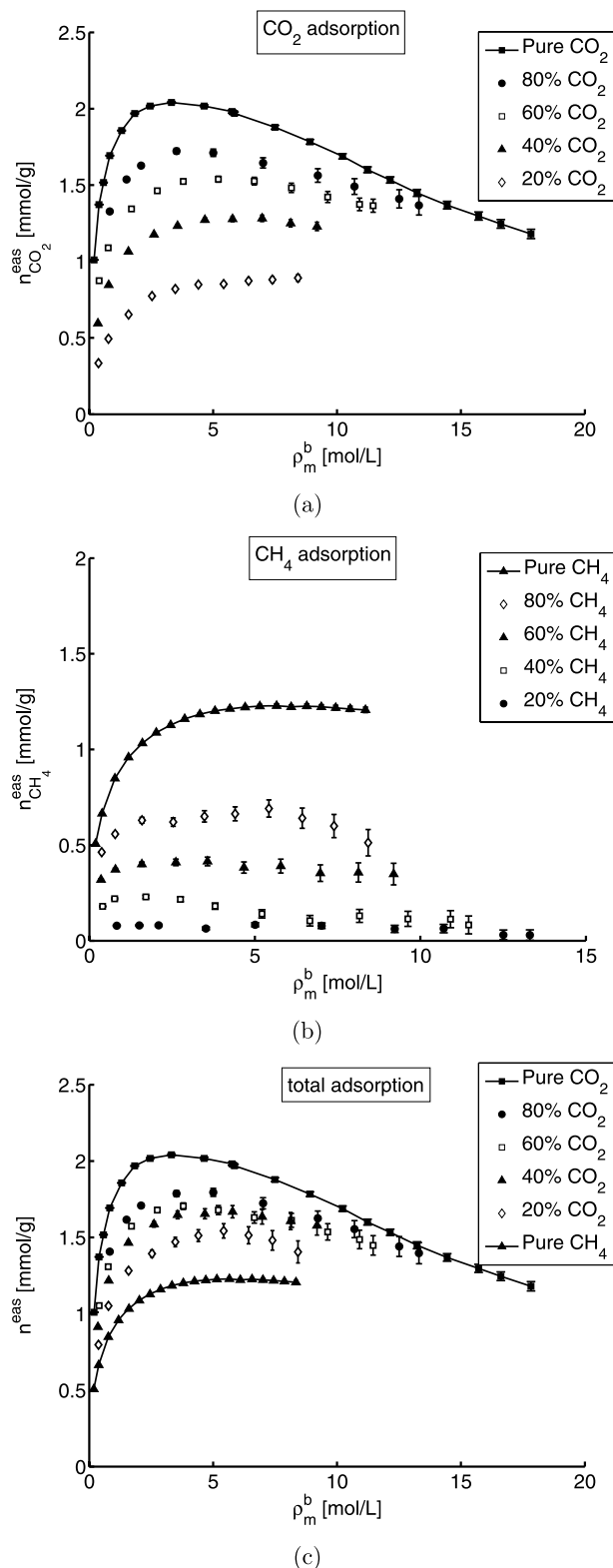
Fig. 5 Individual and total molar excess adsorption and sorption per unit mass of coal for pure CO_2, CH_4 and the four CO_2/CH_4 mixtures on Sulcis coal at a temperature of 45 °C as a function of the molar bulk density ρ_m^b. (**a**), (**b**) and (**c**) represent the CO_2, CH_4 and total molar excess adsorption and sorption, respectively. The data points of the pure CO_2 and CH_4 isotherms are connected to guide the eye

windows, which are orthogonal to the axis of the cylinder, are mounted at its two ends. The view cell is immersed in a water bath and is equipped with a pressure transducer. The measurements are done by direct visualization, i.e. by taking a picture of the coal disc with a digital photo camera.

3.2 Experimental procedure

The experimental procedure has been described in detail in previous publications (Rajendran et al. 2005; Bonavoglia et al. 2006). Nevertheless, the most important steps of the data reconciliation as well as the equations to determine the degree of swelling are summarized here.

The coal disc is placed on a brass holder, which is then positioned inside the view cell. The role of the brass holder is two-fold: first, it ensures to keep the coal disc in a horizontal position and secondly, it is taken as a reference in the evaluation of the coal diameter from the digital picture since its diameter will not be influenced by the fluid pressure. Then, the view cell is brought to the desired temperature and filled up to a certain pressure with the fluid to measured. The coal disc is allowed to expand for two days to reach equilibrium conditions before a picture is taken and the diameter of the disc is determined using a commercial image analysis software. The swelling s is defined as follows

$$s = \frac{V^{coal} - V_0^{coal}}{V_0^{coal}} = \frac{V^s}{V_0^{coal}}, \tag{20}$$

where V_0^{coal} and V^{coal} are initial and final volumes of the coal disc, respectively. The difference $V^{coal} - V_0^{coal}$ corresponds to the volume of the sorbed phase V^s, i.e. the volume increase of the coal due to sorption. In order to calculate the volume of the swollen disc, isotropic expansion is assumed and the swelling s is therefore calculated using the following expression:

$$s(\rho^b, T) = \frac{d^3(\rho^b, T)}{d_0^3} - 1, \tag{21}$$

where d_0 and d represent the initial and final diameters of the coal disc, respectively. Finally, the pressure inside the view cell is increased to a higher level and the described procedure is repeated.

3.3 Results

Using the view cell, measurements of swelling were carried out using the three pure fluids CO_2, CH_4 and He at a temperature of 45 °C and up to a pressure of 130 bar. Additionally, for CO_2 the swelling was measured also at a higher temperature, namely at 60 °C. All the experimental data of swelling
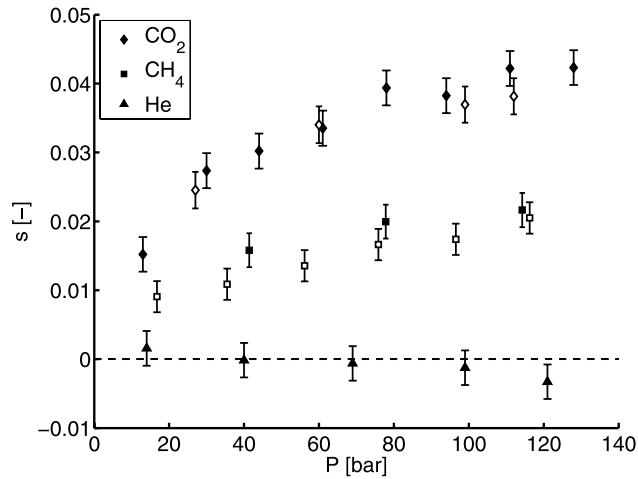
Fig. 6 Swelling s of a Sulcis coal disc under CO_2, CH_4 and He at a temperature of $45\,°C$ as a function of the pressure P. Filled symbols correspond to the first exposure, whereas the empty symbols to the second one
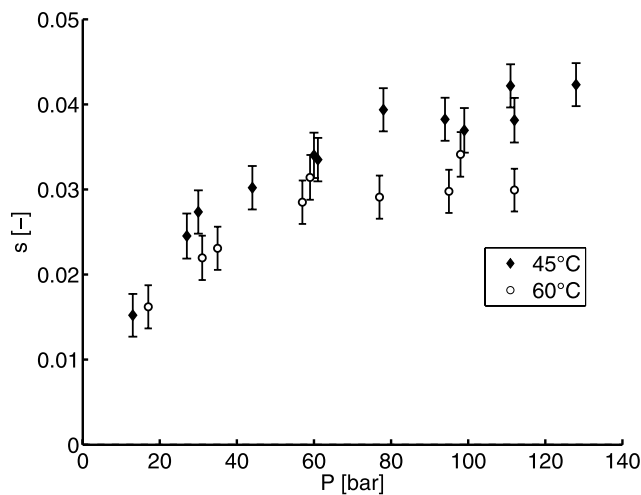
Fig. 7 Influence of temperature on swelling s of a Sulcis coal disc under a CO_2 atmosphere as a function of the pressure P

are reported in Table 4. The direct visualization method applied in this work allowed us calculating the swelling with a precision shown by the error bars in Figs. 6 and 7. These error bars account for the fact that the diameter of the coal disc can only be determined with a precision of 1 pixel.

In Fig. 6 the isotropic swelling s is shown as a function of the pressure P for CO_2 and CH_4 at a temperature of $45\,°C$ and compared to the corresponding swelling under He. The following observations can be made: first, as can be seen from this figure the coal disc was subjected to CO_2 and CH_4 twice and no significant difference has been detected between the two runs. Therefore, it can be concluded that the coal behaves in an equal manner when exposed the second time to CO_2 or CH_4. Secondly, coal swelling increases monotonically with increasing pressure for the fluids CO_2

and CH_4, which have shown a significant excess adsorption and sorption in Sect. 2.4. From these two fluids, CO_2 swells the coal more than methane and shows a maximum swelling of about 4%, whereas the latter reaches swelling ratios of about 2%. Helium, a non-adsorbing fluid, shows a negligible to slightly negative swelling over the same pressure range. A negative swelling could, in principle, be due to matrix compression, even though its extent is extremely small. These results are also in good agreement with the literature, similar results were also found on a coal sample from the South Island, New Zealand (St. George and Barakat 2001). Consequently, the injection of more-swelling fluid CO_2 and the concurrent displacement of the less-swelling fluid CH_4 leads to a net swelling in a potential application of CO_2-ECBM recovery.

Figure 7 presents the influence of temperature on the degree of swelling of the coal disc under CO_2, where the swelling s is plotted as a function of the pressure P for two temperatures 45 and $60\,°C$. It can be seen that the degree of swelling decreases with increasing temperature, as expected.

4 Discussion

As previously anticipated, it is known that gases like CO_2 and CH_4 are able to adsorb on the coal surface, but also to dissolve into its structure causing the coal to swell. On the one hand, the presence of these two processes makes the coal a challenging material to be studied, in particular with respect to the understanding of the fundamental, thermodynamic aspects of adsorption. On the other hand, the study of the adsorption of these gases on coal has a specific practical target, i.e. the prediction of its behavior during an ECBM operation. The amount of CO_2 stored in the seam together with the dynamics of the CO_2/CH_4 displacement represents two main practical aspects to be understood. It is therefore crucial to address these two issues, the theoretical and the practical one, with respect to the experimental data obtained in this work.

4.1 Fundamental study of adsorption

A complete thermodynamic characterization of the adsorption on coal would be achieved with the knowledge of all the variables involved in the process, namely the molar excess amount adsorbed n^{ex}, the amount dissolved n^s and the corresponding swelling s. However, this objective can be partly attained using the experimental techniques presented in this work. In the case of a pure gas, inserting (20) into (9) and after rearrangement, the following expression is obtained:

$$n^{ex} + n^s = n^{eas}(\rho^b, T) + \frac{\rho^b V_{10}^{coal}}{M_m m_{10}^{coal}} s(\rho^b, T). \qquad (22)$$

The right-hand side of this equation contains the variables which can be obtained experimentally, in particular $n^{eas}(\rho^b, T)$ and $s(\rho^b, T)$ from the adsorption and swelling experiments, respectively. Unfortunately, the combination of these two techniques does not allow us to discern between the excess adsorbed amount and the dissolved amount, since only their sum can be calculated. It is worth pointing out that in the case of coal swelling without sorption, i.e. $n^s = 0$ (see Introduction), the adsorption and swelling experiment would be sufficient to completely characterize the adsorption process, since n^{ex} would then be easily obtained through (22).

The same kind of correction could, in principle, also be done for a mixture. Inserting (20) into (17) and after rearrangement, the following expression is obtained:

$$n_i^{ex} + n_i^s = n_i^{eas}(\rho^b, T) + \frac{w_i^b \rho^b V_0^{coal}}{M_{m,i} m_0^{coal}} s(\rho^b, T). \tag{23}$$

In contrast to the pure gases, swelling data of CO_2–CH_4 mixtures are not available, and therefore would have to be estimated from the pure gas. Apart from that, also in the case of a mixture, the conclusion has to be drawn that it is impossible to determine the single quantities n_i^{ex} and n_i^s from the combination of the applied experimental techniques.

4.2 Gas storage capacity

Beside the amount of CH_4 recovered, the main objective of an ECBM project is to store as much CO_2 as possible. Neglecting the presence of water, the CO_2 is stored in the coal seam in three different forms, namely adsorbed on the surface, dissolved in the coal matrix and as a free gas in the pores and cleats (fractures). The estimation of the amount stored in the coal seam follows the same approach used for the calculation of the amount of gas fed to the measuring cell during the adsorption experiments. For obvious reasons and neglecting the presence of leaks, this quantity corresponds exactly to the amount stored in the measuring cell. Rearrangement of (16) gives:

$$m_i^o = w_i^o m^o = m_i^{eas}(\rho^b, T) + w_i^b \rho^b V_0^{void}, \tag{24}$$

where m_i^o, m^o and w_i^o correspond to the individual and total mass of gas stored and its corresponding mass fraction, respectively. V_0^{void} corresponds to the volume accessible to the gas when the coal is in its unswollen state and therefore, in the case of a coal seam, it corresponds to the volume of the pores including fractures. Dividing (24) by $M_{m,i} m_0^{coal}$, using the definition of the bulk weight fraction, $w_i^b = y_i^b M_{m,i} / \sum_{i=1}^{N} y_i^b M_{m,i}$, and inserting (19) for the molar bulk density ρ_m^b yields the molar amount of component i

stored per unit mass of coal:

$$n_i^o = n_i^{eas}(\rho_m^b, T) + y_i^b \rho_m^b \frac{V_0^{void}}{m_0^{coal}}. \tag{25}$$

Note that this equation simplifies to the one presented in the literature for a non-sorbing and therefore non-swelling system (Sircar 1985a) by setting n_i^{eas} equal to the molar excess adsorption n_i^{ex}.

The porosity ε of the coal seam is related to the void volume V^{void} and the bulk density of the coal ρ_s^b, i.e. the mass of coal per unit volume of the coal seam, by the following relationship:

$$\varepsilon(V^{void}) = \frac{V^{void} \rho_s^b}{m_0^{coal}}. \tag{26}$$

Equation 25 can now be transformed into a more convenient form by using (26) expressed for the initial porosity ε^0 of the unswollen coal seam:

$$n_i^o = n_i^{eas}(\rho_m^b, T) + \frac{y_i^b \rho_m^b \varepsilon^0}{\rho_s^b}. \tag{27}$$

Therefore, the information required to estimate the amount of gas stored in the coal seam is the isotherms $n_i^{eas}(\rho_m^b, T)$ obtained directly from the adsorption experiments, the bulk mole fraction y_i^b with its molar density ρ_m^b, the bulk density of the adsorbent ρ_s^b and the initial porosity ε^0. It is worth noting that no information about the swelling is needed.

4.3 Coal seam dynamics

The amount of CH_4 recovered, the time needed for the CO_2 to break through at the production well or injection policies are some important issues to be addressed before starting an ECBM project. A model which describes the dynamics of the CO_2/CH_4 displacement in the coal seam has to be used to predict these quantities and assess the potential of the ECBM operation. Moreover, this model should contain the information gained from the experiments in the laboratory, i.e. the multicomponent adsorption isotherms on coal, swelling behavior of the coal, etc. A way to start with is to treat the coal seam as a column packed with an adsorbent which in our case is coal. The equations describing this kind of system have been derived in the literature in terms of excess properties (Sircar 1985b). They base on the assumption of no surface flow in the adsorbed phase. The mass balance over a differential section of the column leads to the following equation:

$$\rho_s^b \frac{\partial n_i^o}{\partial t} = -\frac{\partial(Q y_i^b)}{\partial x}, \tag{28}$$

where n_i^o is the total amount of component i at a position x and at a time t, and Q is the molar gas flow rate per unit

cross-sectional area. Expressing the latter in terms of the molar bulk density ρ_m^b and the superficial velocity u, namely $Q = \rho_m^b u$, and using the definition of n_i^o given previously, (28) can be rearranged as:

$$\rho_s^b \frac{\partial n_i^{eas}(\rho_m^b, T)}{\partial t} + \varepsilon^0 \frac{\partial}{\partial t}\left(\rho_m^b y_i^b\right) = -\frac{\partial\left(\rho_m^b u y_i^b\right)}{\partial x}. \qquad (29)$$

The left-hand side of this equation, i.e. the accumulation term, contains quantities which can be directly obtained experimentally and are independent of swelling, as explained in the previous section. In the convection term, however, the swelling will affect the porosity and as a consequence the superficial velocity u which therefore cannot be taken as a constant. The flow in a porous medium is often described using Darcy's law, which in its simplest form relates u to the pressure gradient through the bed as follows:

$$u = -\frac{k}{\mu}\frac{\partial P}{\partial x}, \qquad (30)$$

where k and μ correspond to the permeability and the viscosity, respectively. The information about the change in porosity caused by swelling is contained in the permeability term. In this case, it is therefore needed to implement the swelling data obtained from the experiments in a geomechanical model for the description of the porosity and permeability of the coal seam. Having this information, the model then completely characterizes the dynamics of the coal seam.

5 Nomenclature

a	Peak area fraction from gas chromatography analysis [–]
A	Adsorbent surface area [cm^2]
d	Diameter of coal disc [cm]
k	Permeability [cm^2]
m	Mass [g]
m^{eas}	Excess mass adsorbed and sorbed [g]
m^{ex}	Excess mass adsorbed [g]
M_m	Molar mass of adsorbate [g/mol]
$\mathcal{M}_1$	Weight at measuring point 1 [g]
$\mathcal{M}_1^0$	Weight at measuring point 1 under vacuum [g]
$\mathcal{M}_2$	Weight at measuring point 2 [g]
n^{eas}	Molar excess adsorption and sorption per unit mass of coal [mmol/g]
n^{ex}	Molar excess adsorption per unit mass of coal [mmol/g]
N	Number of components in the mixture [–]
P	Pressure [bar]
Q	Molar gas flow rate per unit cross-sectional area [mol/(cm^2 s)]

R_o	Vitrinite reflectance coefficient [–]
s	Swelling [–]
t	Time [s]
T	Temperature [K]
u	Superficial velocity [cm/s]
V	Volume [cm^3]
V^0	Volume of lifted metal parts and coal sample 1 [cm^3]
V_1^*	Volume of stainless steel cylinder 1 [cm^3]
V_2^*	Volume of stainless steel cylinder 2 [cm^3]
V^{void}	Void volume of adsorption system [cm^3]
w_i	Mass fraction of component i in the mixture [–]
x	Column axis [cm]
y_i	Mole fraction of component i in the mixture [–]
z	Axis perpendicular to adsorbent surface [cm]

Greek letters

ε	Porosity [cm^3 void/cm^3 column]
μ	Viscosity [Pa s]
ρ	Density [g/cm^3]
ρ_1	Density before expansion [g/cm^3]
ρ_2	Density after expansion [g/cm^3]
ρ_m	Molar density [mol/L]
ρ_s^b	Bulk density of the adsorbent [g/cm^3]

Subscripts and superscripts

a	Adsorbed
b	Bulk
c	Critical
coal	Coal sample
feed	Feed
He	Helium
i	Component i
met	Lifted metal parts
o	Stored
s	Sorbed
sinker	Sinker element
*	Stainless steel cylinder
0	Initial
1	Magnetic suspension balance
2	Auxiliary adsorption cell

Appendix A: Determination of the void volume

The adsorption measurements require that the void volume, V_0^{void}, of the adsorption system, i.e. the volume accessible to the gas, is known (see Sect. 2.4). There are different ways to calibrate the volume of the system. One possibility is to fill a vessel, whose volume is precisely known, with gas and to expand it into the volume to be calibrated. Another possibility is to fill the volume to be calibrated with a pressurized gas, to measure its density and to determine the amount of gas with a flowmeter while expanding it to atmospheric conditions. In this work, a third method has been adopted, which is described below. As shown in Fig. 1, the volume to be calibrated reaches valve V12, and it consists of two parts separated by valves V11 and V13, i.e. volume V_1 containing the measuring cell of the magnetic suspension balance and volume V_2 containing the auxiliary adsorption cell, the circulation pump and switching valve I.

The calibration is performed when the adsorbent is not present in the system. After evacuating the whole adsorption system at a temperature of 45 °C, the volume V_1 is filled with argon at a pressure up to 200 bar, let equilibrate and the density ρ_1 is measured. Then, the gas is expanded into the volume V_2 and the resulting density ρ_2 is measured. The amount of gas in the system remains constant and therefore the following relationship holds:

$$V_1 \rho_1 = (V_1 + V_2) \rho_2. \tag{31}$$

The procedure is repeated several times at different density levels to increase the accuracy of the volume calibration. For the expansion experiments, argon is used due to the resulting larger density changes as compared to helium.

In a second step, two stainless steel cylinders of known dimensions are introduced in the auxiliary cell and the expansion experiments are repeated. The volumes of the cylinders are $V_1^* = 38.7$ cm^3 and $V_2^* = 46.0$ cm^3, respectively. The dimensions are chosen such that they fit exactly into the auxiliary cell. The amount of gas before and after the expansion is now given by:

$$V_1 \rho_1^* = (V_1 + V_2 - V_1^* - V_2^*) \rho_2^*, \tag{32}$$

where ρ_1^* and ρ_2^* are the densities before and after the expansion, respectively. From (31) and (32) the two unknowns V_1 and V_2 are easily obtained: $V_1 = 148.75 \pm 0.08$ cm^3 and $V_2 = 153.99 \pm 0.02$ cm^3. The void volume V_0^{void} of the coal in its unswollen state that applies during the adsorption measurements is obtained by accounting for the initial coal volume V_0^{coal} as

$$V_0^{\text{void}} = V_1 + V_2 - V_0^{\text{coal}} - V_1^*, \tag{33}$$

where only the stainless steel cylinder of volume V_2^* has been removed from the adsorption cell. We have obtained $V_0^{\text{void}} = 234.14 \pm 0.12$ cm^3.

Appendix B: Error estimation

In the present study, the errors in the measured excess adsorption and sorption are estimated through the method of error propagation, which is also confirmed through repetitive measurements. The density of the fluid is obtained from the following equation

$$\rho^{\text{b}} = \frac{m_0^{\text{sinker}} - \mathcal{M}_2(\rho^{\text{b}}, T) + \mathcal{M}_1(\rho^{\text{b}}, T)}{V^{\text{sinker}}}, \tag{34}$$

where $\mathcal{M}_1(\rho^{\text{b}}, T)$ and $\mathcal{M}_2(\rho^{\text{b}}, T)$ correspond to the signal of the balance in the first and the second position, while m_0^{sinker} and V^{sinker} are the mass and volume of the calibrated sinker, respectively. The error in the density is then defined as:

$$\Delta \rho^{\text{b}} = \left[\left(\frac{\partial \rho^{\text{b}}}{\partial m_0^{\text{sinker}}} \Delta m_0^{\text{sinker}} \right)^2 \right.$$
$$+ \left(\frac{\partial \rho^{\text{b}}}{\partial \mathcal{M}_2(\rho^{\text{b}}, T)} \Delta \mathcal{M}_2(\rho^{\text{b}}, T) \right)^2$$
$$+ \left(\frac{\partial \rho^{\text{b}}}{\partial \mathcal{M}_1(\rho^{\text{b}}, T)} \Delta \mathcal{M}_1(\rho^{\text{b}}, T) \right)^2$$
$$\left. + \left(\frac{\partial \rho^{\text{b}}}{\partial V^{\text{sinker}}} \Delta V^{\text{sinker}} \right)^2 \right]^{0.5}, \tag{35}$$

where $\Delta m_0^{\text{sinker}}$ and ΔV^{sinker} are the errors with which the mass and the volume of the sinker are known. The errors $\Delta \mathcal{M}_1$ and $\Delta \mathcal{M}_2$ are both equal to the accuracy $\Delta \mathcal{M}$ of the magnetic suspension balance. Using (34), the following relationship describing the measurement error on the density is obtained,

$$\Delta \rho^{\text{b}} = \left[\left(\frac{\Delta m_0^{\text{sinker}}}{V^{\text{sinker}}} \right)^2 + 2 \left(\frac{\Delta \mathcal{M}}{V^{\text{sinker}}} \right)^2 \right.$$
$$\left. + \left(\frac{\Delta V^{\text{sinker}}}{V^{\text{sinker}}} \rho^{\text{b}} \right)^2 \right]^{0.5} \tag{36}$$

which is supplemented with the following information from the calibration certificate of the balance:

$$\Delta m_0^{\text{sinker}} = 0.00001 \text{ g},$$
$$V^{\text{sinker}} = 4.22555 \text{ cm}^3,$$
$$\Delta V^{\text{sinker}} = 0.00211 \text{ cm}^3,$$
$$\Delta \mathcal{M} = 0.00005 \text{ g}.$$

The error on the molar excess adsorption and sorption Δn_i^{eas} is then determined in a similar fashion as for the density of the fluid, namely using (1) to (3) and (8) to (18) listed in

Sects. 2.3 and 2.4, respectively. The derivation is extensive, but not mathematically demanding. Therefore, the complete derivation of the error propagation is omitted here for the sake of a better readability. The required errors in the coal masses and in the void volume of the system are given below:

$$\Delta m_{10}^{coal} = 0.0001 \text{ g},$$

$$\Delta m_{20}^{coal} = 0.01 \text{ g},$$

$$\Delta V_0^{void} = 0.12 \text{ cm}^3,$$

$$\frac{\Delta w_{CH_4}}{w_{CH_4}} = 0.1\%$$

The error related to the gas phase composition determined by gas chromatography analysis was estimated from repetitive injections and finally the resulting estimated errors are shown in terms of error bars in Figs. 2 to 5.

References

Arri, L.E., Yee, D., Morgan, W.D., Jeansonne, M.W.: Modeling coalbed methane production with binary gas sorption. SPE Paper 24363, Presented at the SPE Rocky Mountain Regional Meeting, Casper, Wyoming, May 18–21, 1992

Bae, J.S., Bhatia, S.K.: High-pressure adsorption of methane and carbon dioxide on coal. Energy Fuels **20**, 2599–2607 (2006)

Bonavoglia, B., Storti, G., Morbidelli, M., Rajendran, A., Mazzotti, M.: Sorption and swelling of semicrystalline polymers in supercritical CO_2. J. Polym. Sci. Part B Polym. Phys. **44**, 1531–1546 (2006)

Busch, A., Gensterblum, Y., Krooss, B.M.: Methane and CO_2 sorption and desorption measurements on dry Argonne premium coals: pure components and mixtures. Int. J. Coal Geol. **55**, 205–224 (2003)

Busch, A., Gensterblum, Y., Krooss, B.M., Siemons, N.: Investigation of high-pressure selective adsorption/desorption CO_2 and CH_4 on coals: An experimental study. Int. J. Coal Geol. **66**, 53–68 (2006)

Ceglarska-Stefanska, G., Zarebska, K.: Sorption of carbon dioxide-methane mixtures. Int. J. Coal Geol. **62**, 211–222 (2005)

Chaback, J.J., Morgan, W.D., Yee, D.: Sorption of nitrogen, methane, carbon dioxide and their mixtures on bituminous coals at in-situ conditions. Fluid Phase Equilib. **117**, 289–296 (1996)

DeGance, A.E., Morgan, W.D., Yee, D.: High-Pressure Adsorption of Methane, Nitrogen and Carbon-Dioxide on Coal Substrates. Fluid Phase Equilib. **82**, 215–224 (1993)

Di Giovanni, O., Dörfler, W., Mazzotti, M., Morbidelli, M.: Adsorption of supercritical carbon dioxide on silica. Langmuir **17**, 4316–4321 (2001)

Dreisbach, F., Staudt, R., Keller, J.U.: High pressure adsorption data of methane, nitrogen, carbon dioxide and their binary and ternary mixtures on activated carbon. Adsorption **5**, 215–227 (1999)

Dreisbach, F., Seif, R., Lösch, H.W.: Gravimetric measurement of adsorption equilibria of gas mixture CO/H_2 with a magnetic suspension balance. Chem. Eng. Technol. **25**, 1060–1065 (2002)

Fitzgerald, J.E., Pan, Z., Sudibandriyo, M., Robinson, R.L. Jr., Gasem, K.A.M., Reeves, S.: Adsorption of methane, nitrogen, carbon dioxide and their mixtures on wet Tiffany coal. Fuel **84**, 2351–2363 (2005)

Fitzgerald, J.E., Robinson, R.L. Jr., Gasem, K.A.M.: Modeling high-pressure adsorption of gas mixtures on activated carbon and coal using a simplified local-density model. Langmuir **22**, 9610–9618 (2006)

Harpalani, S., Schraufnagel, R.A.: Shrinkage of coal matrix with release of gas and its impact on permeability of coal. Fuel **69**, 551–556 (1990)

Hocker, T., Rajendran, A., Mazzotti, M.: Measuring and Modeling Supercritical adsorption in porous solids. Carbon dioxide on 13X zeolite and on silica gel. Langmuir **19**, 1254–1267 (2003)

IPCC: IPCC Special Report on Carbon Dioxide Capture and Storage. Cambridge University Press, Cambridge (2005)

IPCC, Climate Change 2007: The Physical Science Basis. Summary for Policymakers. Contribution of Working Group I to the Fourth Assessment Report of the Intergovernmental Panel on Climate Change, available online at http://www.ipcc.ch (2007)

Karacan, C.O.: Heterogeneous sorption and swelling in a confined and stressed coal during CO_2 injection. Energy Fuels **17**, 1595–1608 (2003)

Keller, J.U., Staudt, R.: Gas Adsorption Equilibria: Experimental Methods and Adsorptive Isotherms. Springer, New York (2005)

Keller, J.U., Dreisbach, F., Rave, H., Staudt, R., Tomalla, M.: Measurement of gas mixture adsorption equilibria of natural gas compounds on microporous sorbents. Adsorption **5**, 199–214 (1999)

Krooss, B.M., van Bergen, F., Gensterblum, Y., Siemons, N., Pagnier, H.J.M., David, P.: High-pressure methane and carbon dioxide adsorption on dry and moisture-equilibrated Pennsylvanian coals. Int. J. Coal Geol. **51**, 69–92 (2002)

Larsen, J.W.: The effects of dissolved CO_2 on coal structure and properties. Int. J. Coal Geol. **57**, 63–70 (2004)

Mazumder, S., van Hemert, P., Busch, A., Wolf, K.-H.A.A., Tejera-Cuesta, P.: Flue gas and pure CO_2 sorption properties of coal: A comparative study. Int. J. Coal Geol. **67**, 267–279 (2006)

Milewska-Duda, J., Duda, J., Nodzenski, A., Lakatos, J.: Absorption and adsorption of methane and carbon dioxide in hard coal and active carbon. Langmuir **16**, 5458–5466 (2000)

Ottiger, S., Pini, R., Storti, G., Mazzotti, M., Bencini, R., Quattrocchi, F., Sardu, G., Deriu, G.: Adsorption of pure carbon dioxide and methane on dry coal from the Sulcis Coal Province (SW Sardinia, Italy). Environ. Prog. **25**, 355–364 (2006)

Pan, Z., Connell, L.D.: A theoretical model for gas adsorption-induced coal swelling. Int. J. Coal Geol. **69**, 243–252 (2007)

Pini, R., Ottiger, S., Rajendran, A., Storti, G., Mazzotti, M.: Reliable measurement of near-critical adsorption by gravimetric method. Adsorption **12**, 393–403 (2006)

Quattrocchi, F., Bencini, R., Amorino, C., Basili, R., Caddeo, G., Cantucci, B., Cara, R., Cauli, G., Cinti, D., Deidda, C., Deriu, G., Fadda, A., Fadda, M., Fandino, V., Faranzena, S., Giannelli, A., Galli, G., Mazzotti, M., Ottiger, S., Pizzino, L., Pini, R., Sardu, G., Storti, G., Voltattorni, N.: Feasibility study (I stage) of CO_2 geological storage by ECBM techniques in the Sulcis coal province (SW Sardinia, Italy). In Proceedings of the 8th International Conference on Greenhouse Gas Control Technologies, Trondheim, Norway, June 19–22, 2006

Rajendran, A., Bonavoglia, B., Forrer, N., Storti, G., Mazzotti, M., Morbidelli, M.: Simultaneous measurement of swelling and sorption in a supercritical CO_2-poly(methyl methacrylate) system. Ind. Eng. Chem. Res. **44**, 2549–2560 (2005)

Reeves, S., Taillefert, A., Pekot, L., Clarkson, C.: The Allison unit CO_2-ECBM pilot: a reservoir modeling study. Topical report, US Department of Energy, available online at http://coal-seq.com (2003)

Reucroft, P.J., Sethuraman, A.R.: Effect of pressure on carbon-dioxide induced coal swelling. Energy Fuels **1**, 72–75 (1987)

Scherer, G.W.: Dilatation of porous-glass. J. Am. Ceram. Soc. **69**, 473–480 (1986)

Shimada, S., Li, H.Y., Oshima, Y., Adachi, K.: Displacement behavior of CH_4 adsorbed on coals by injecting pure CO_2, N_2, and CO_2–N_2 mixture. Environ. Geol. **49**, 44–52 (2005)

Sircar, S.: Excess properties and thermodynamics of multicomponent gas adsorption. J. Chem. Soc. Faraday Trans. I **81**, 1527–1540 (1985a)

Sircar, S.: Excess properties and column dynamics of multicomponent gas adsorption. J. Chem. Soc. Faraday Trans. I **81**, 1541–1545 (1985b)

St. George, J.D., Barakat, M.A.: The change in effective stress associated with shrinkage from gas desorption in coal. Int. J. Coal Geol. **45**, 105–113 (2001)

Stevenson, M.D., Pinczewski, W.V., Somers, M.L., Bagio, S.E.: Adsorption/desorption of multicomponent gas mixtures at in-seam conditions. SPE Paper 23026, Presented at the SPE Asia-Pacific Conference, Perth, Western Australia, November 4–7, 1991

Van Bergen, F.: Field experiment of CO_2-ECBM in the upper Silesian basin of Poland. Presented at the 5th International Forum on Geologic Sequestration of CO_2 in Deep, Unmineable Coalseams (Coal-Seq V), Houston TX, November 8–9, 2006

Wong, S., Law, D., Deng, X., Robinson, J., Kadatz, B., Gunter, W.D., Ye, J., Feng, S., Fan, Z.: Enhanced coalbed methane—micro-pilot test at South Qinshui, Shanxi, China. In Proceedings of the 8th International Conference on Greenhouse Gas Control Technologies, Trondheim, Norway, June 19–22, 2006

Yamaguchi, S., Ohga, K., Fujioka, M., Nako, M., Muto, S.: Field experiment of Japan CO_2 geosequestration in coal seams project (JCOP). In Proceedings of the 8th International Conference on Greenhouse Gas Control Technologies, Trondheim, Norway, June 19–22, 2006

Zehnder, B.: NIR-spektroskopische Bestimmung von Stoffaustauschkoeffizienten und Gleichgewichtslöslichkeiten in Fluid-Fluid-Systemen unter überkritischen Bedingungen. Dissertation Nr. 9657. ETH Zurich, Switzerland (1992)